JEOFİZİK 15, 3-17, 2001

DEEP STRUCTURE OF NE TUZ LAKE, CENTRAL ANATOLIA, FROM POTENTIAL FIELD, SEISMIC, BOREHOLE AND OTHER GEOPHYSICAL AND GEOLOGICAL DATA

Potansiyel Alan, Sismik, Kuyu ve Diğer Jeofizik ve Jeolojik Verilerden Orta Anadolu, Tuz Gölü KD Kesiminin Derin Yapısı

Abdullah ATEŞ[1] and Philip KEAREY[2]

ABSTRACT

The NE Tuz Lake is located in a tectonically non-active region, but is surrounded by major tectonic features. The gravity and aeromagnetic fields of the NE Tuz Lake region show large positive anomalies which appear to be not coincident . The surface geology does not indicate causative sources for these anomalies neither. A seismic reflection profile close to a borehole is used to construct two-dimensional gravity and magnetic models in the NE-SW direction. Gravity and magnetic models are explained by a deep seated high density and susceptibility body of gabbroic origin. Pseudogravity transformation of magnetic anomalies with correct body magnetization indicates that the body causing the gravity and magnetic anomalies may have the same origin. Shape analysis suggests that the body causing the gravity and magnetic anomalies appear to be affected by the main Palaeo-Tethyan suture. Analysis of the aeromagnetic anomalies also suggests that the causative body gained remanent magnetization during a reverse polarity era before the anticlockwise rotation of Anatolia and it may, thus, be related to a Palaeo-Tethyan age.

ÖZET

Tuz Gölü'nün KD'su tektonik olarak aktif olmayan, ama önemli kenet kuşakları ile çevrelenmiş bir bölgedir. Bölgeye ait gravite ve manyetik alanlar, birbirleri ile ilişkileri olmayan, şiddeti büyük pozitif anomaliler vermektedir. Yüzey jeolojisinden de anomalilere neden olabilecek kaynak yapılar görülememektedir. Bir sismik kesit ve kuyu verilerinden yararlanılarak, KD-GB doğrultularında iki boyutlu gravite ve manyetik modeller oluşturulmuştur. Gravite ve manyetik modeller kökenleri gabro ve derinden kaynaklanan, yapıların varlığı ile açıklanabilmektedir. Manyetik anomalilerden, düzeltilmiş yapı mıknatıslanması kullanılarak, oluşturulan yapma-gravite dönüşümü gravite ve manyetik anomalilere aynı yapının neden olabileceğini ortaya koymuştur. Gravite ve manyetik anomalilere neden olan yapının Ana Paleo-Tetis kenedinin etkisi altında kaldığı gözlenmektedir. Havadan manyetik anomalilerin analizlerinden sözü edilen yapının Anadolu'nun satin tersi yönündeki dönmesinden önceki bir ters polarite döneminde kalıntı mıknatıslanma kazandığı ileri sürülmektedir.

[1]Ankara Üniversitesi, Jeofizik Mühendisliği Bölümü, Beşevler 06100 Ankara, Turkey.
[2]Department of Earth Sciences, University of Bristol, Bristol BS8 1RJ, England, UK.

TECTONIC SETTING AND SURFACE GEOLOGY

The NE Tuz Lake region is situated centrally in the Kırşehir Block (Fig. 1). The region is surrounded by major tectonic suture zones and micro platelets which were described by Ketin (1966) and later by Şengör (1981). The surface geology, in general, exhibits sedimentary units which may be metamorphosed and intrusive acid and basic rocks (Fig. 2). The surface lithologies appear to extend in a NW-SE direction, parallel to the Inner Tauride Suture. Görür et al. (1984) suggested that geological and geophysical investigations were carried out in the Tuz Lake basin because of its supposed hydrocarbon potential. They also suggested that the Tuz Lake

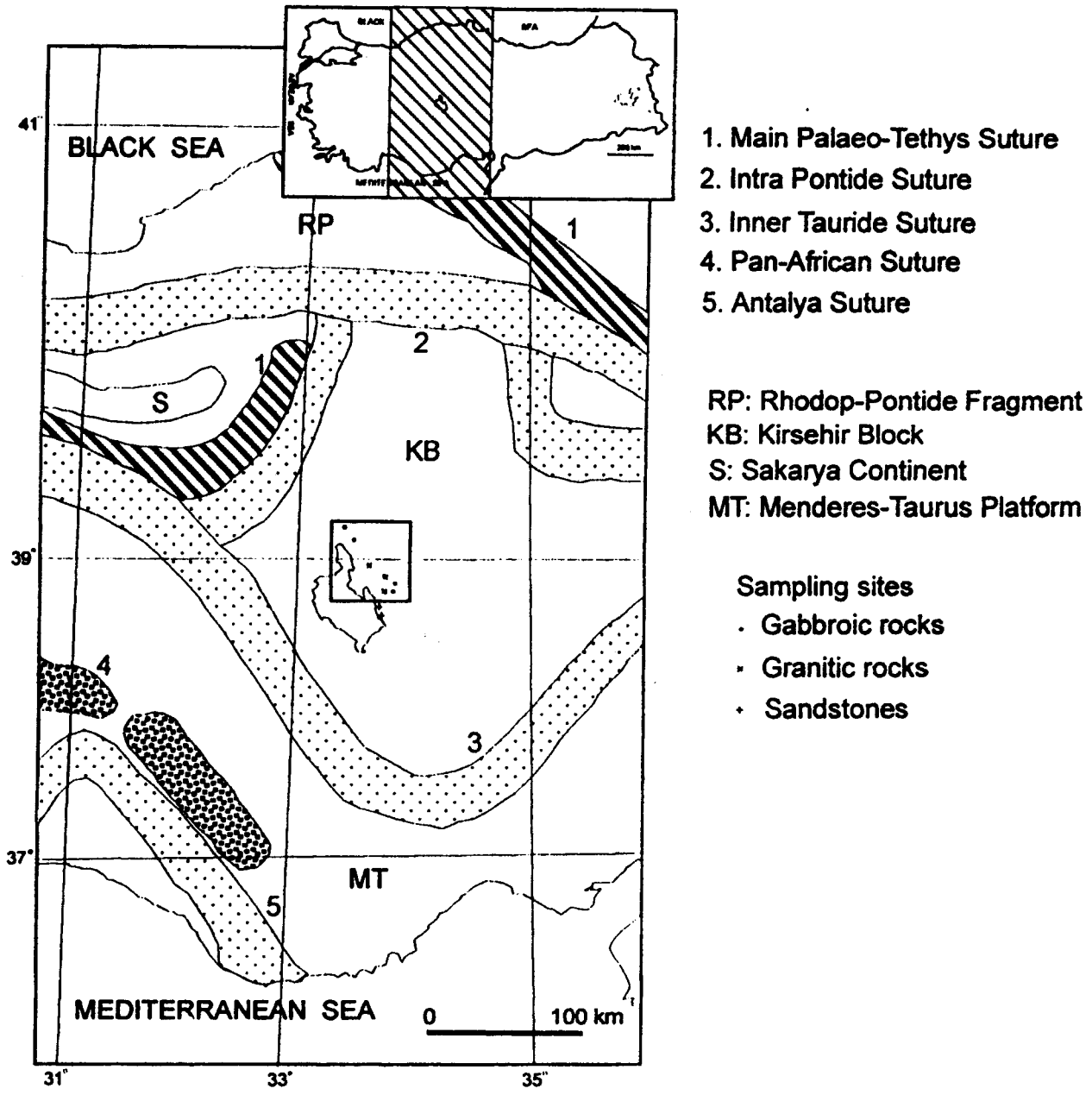

Figure 1. Location map and regional geological setting of the study area. Small box show the research area.

Şekil 1. Çalışma alanının bulduru haritası ve rejyonal jeolojik yerleşkesi. Araştırma alanı küçük kutu içinde gösterilmektedir.

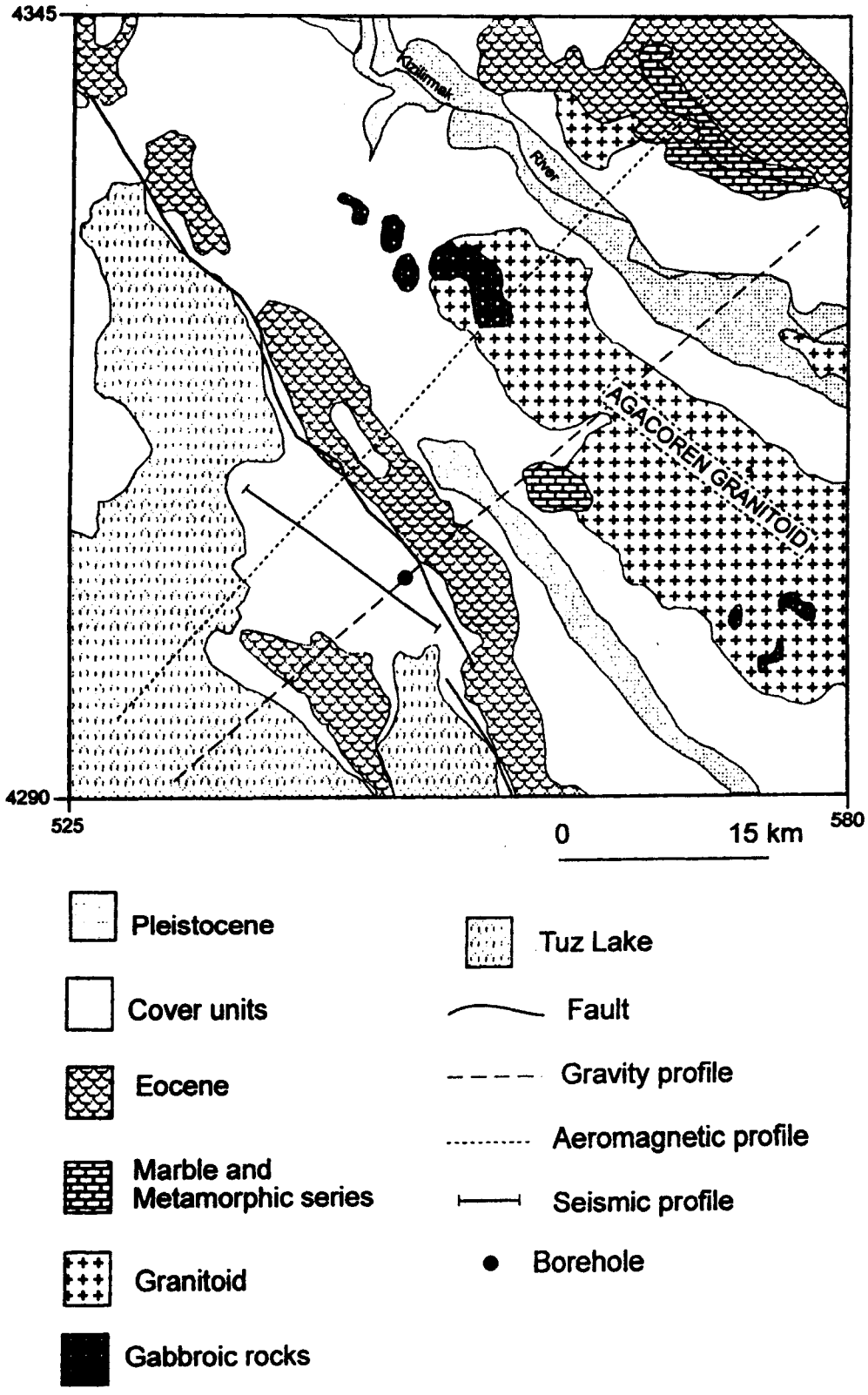

Figure 2. Geological map of the research area (after Erentöz and Ketin 1961, Bingöl 1989).

Şekil 2. Araştırma alanının jeoloji haritası (Erentöz ve Ketin 1961, Bingöl 1989'dan sonra).

region is composed of several basins mixed with each other by the complex tectonic processes of the Alpine orogeny, and thus a satisfactory model for the evolution of the basin could not be found. In the region, the earliest geophysical work was aeromagnetic surveying of some part of Central Anatolia by Hutchison et al. (1962). Kadıoğlu et al. (1998) investigated the small gabbroic outcrops near the southeast corner of the study area. It was suggested from the aeromagnetic modeling that the small outcrops join each other at depth and their root extends down as deep as 9 km.

POTENTIAL FIELD DATA

In central Turkey, north east of Tuz Lake, the aeromagnetic anomaly map of Turkey shows an anomaly almost centered on 33°, 30' E and 39°, 00' N (Ateş et al. 1999). The same anomaly cannot be seen in the gravity anomalies of the same region. This may be caused by the 10 km grid spacing of the regional gravity anomalies.

For the study area shown in Figure 2, gravity and aeromagnetic anomaly data were obtained from the General Directorate of the Mining Research and Exploration of Turkey (MTA) in a digital form. Both data sets were gridded at 2.5 km intervals using a standard gridding routine by MTA. The aeromagnetic data, were obtained at 1 km flight line intervals, 0.6 km above the surface, were corrected for the International Geomagnetic Reference Field (IGRF) using a computer program supplied by Baldwin and Langel (1993). Contoured gravity and aeromagnetic anomaly maps are shown in Figs. 3 and 4, respectively. Gravity anomalies in Figure 3 show a high gradient in the NE of the region, extending NNE-SSW, a low anomaly gradients at the northern end of Tuz Lake and through the NW corner. Aeromagnetic anomalies of the area (Fig. 4) show several high amplitudes at the NE neck of Tuz Lake. The causative source for this anomaly does not appear to be the same source causing the gravity anomaly in Figure 3.

DENSITY AND SUSCEPTIBILITY DATA

13 samples of gabbroic, 11 samples of granite and 17 samples of sandstone (Paleocene-Eocene) rocks were collected from the locations shown in Fig. 1. Gabbroic, granitic and arenitic rocks were collected from the locations marked [•], [x], [+] signs, respectively. Table 1 shows the ranges and average densities of these rock units. Figure 5 shows density histograms of these rock units. Density measurements were made with a Walker's Steelyard Balance when they were brought from the field. Susceptibility measurements were made using a SM-5 Scintrex susceptibility meter. Table 2 shows susceptibilities of the rock samples. Gabbroic rocks gave the highest susceptibility. Granite and sandstone have little or no susceptibility.

POWER SPECTRUM ANALYSES

Power spectrum analysis has been applied to the regions shown by boxes in Figures 3 and 4 according to the method of Spector and Grant (1970). By means of the power spectrum depth to the top of the anomalous body can be estimated by the following equation;

$\bar{h} = \frac{\Delta P}{4\pi\Delta K}$ where $\bar{h}$ is the mean depth to the top of the source body, ΔP is the $\Delta \ln_e$ Power, ΔK is the ΔK wavenumber (km^{-1}).

Both gravity and aeromagnetic power spectra are shown in Figures 6.a and b were fitted with single lines, which can be interpreted as the depths to the bodies causing both gravity and magnetic anomalies are about 2.8 km (Figs. 6.a and b). It can thus, be suggested that the same source body is causing gravity and magnetic anomalies.

SEISMIC REFLECTION AND BORHOLE DATA

A seismic reflection profile (DG-2012) and a borehole (Tuzgölü-1), acquired by the Turkish Petroleum Company, were released by the General Directorate of Petroleum Affairs in Turkey. The location of the reflection line and the borehole are shown in Figure 2. The reflection line has been CDP and NMO processed. Along the reflection line, functions of velocity with depth have also been analysed. Seismic profile DG-2012 and a line drawing are shown in Figures 7 and 8. Seismic reflection profile DG-2012 demonstrates strong reflec-

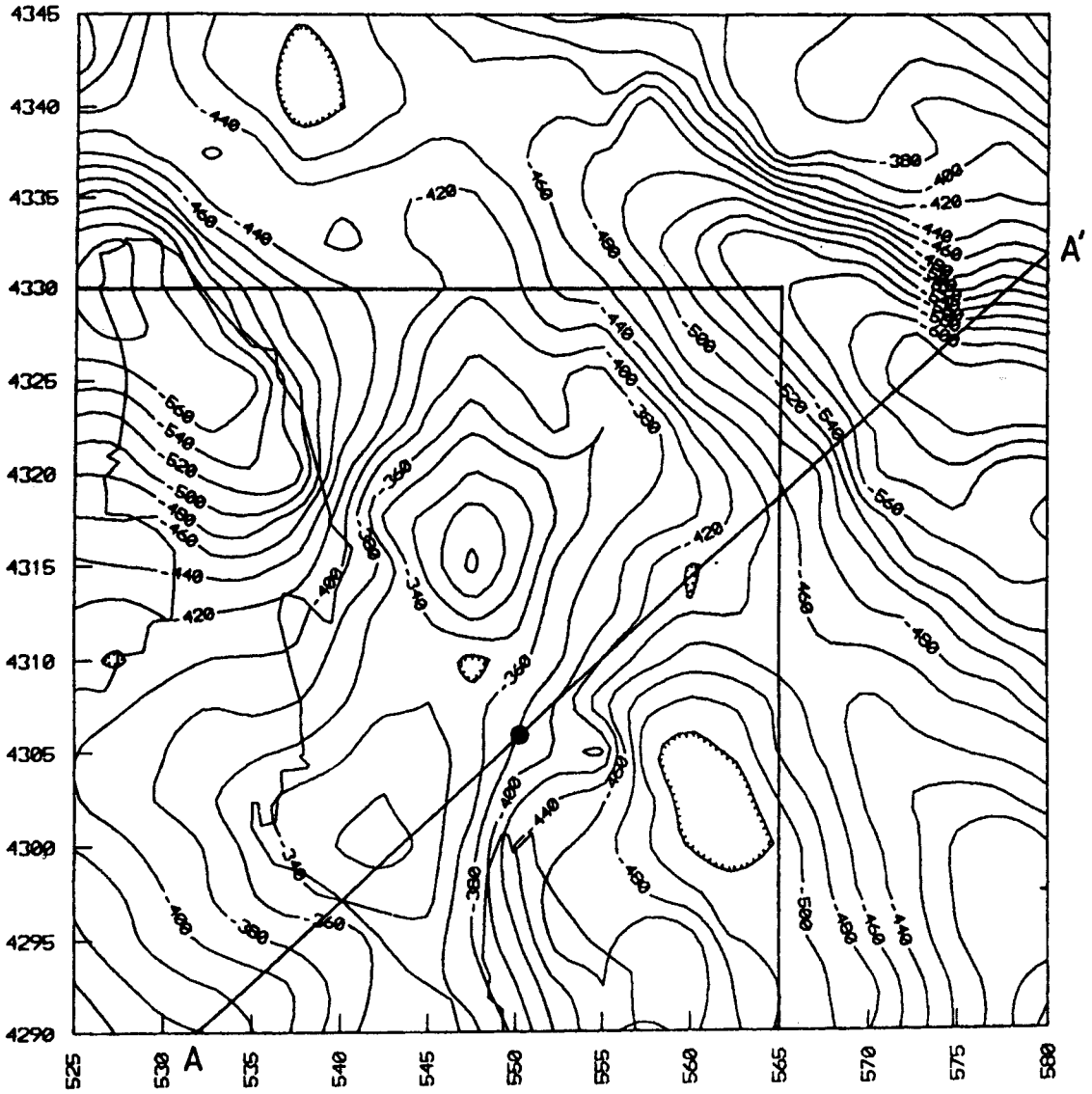

Figure 3. Gravity anomaly map. Contour interval is 20 gu. Power spectrum depth estimate method was applied to the area shown in the box. AA' is the interpreted gravity anomaly profile. Closed circle shows the location of the borehole Tuzgölü-1.

Şekil 3. Gravite anomaly haritası. Kontur aralığı 20 gu'dur. Güç spektrumu derinlik tahmini yöntemi kutu içinde gösterilen bölgeye uygulanmıştır. AA' yorumlanan gravite anomaly profilidir. İçi dolu daire Tuzgölü-1 kuyusunun yerini göstermektedir.

tion events at different levels. Strong reflection groups are labeled as R1 and R2. Velocity analysis suggests that the continuous reflection event, R1, seen from 1.2-1.9 sec. along NW-SE direction can be related to the gabbroic intrusions inferred from gravity and magnetic power spectra. At the middle of the section R1 is at 1.25 sec. from the surface with a velocity of 4400 m/sec. This would provide a depth of 2750 m from surface which is in good agreement with the power spectra depth calculations. Reflections R2 are events dipping NW and mainly dominant at the middle of the section between arrival times of 3 sec. to 5 sec. A depth range of 4.7 km to 13 km is obtained from these times. Since the SE end of the seismic section is close to the gravity anomaly profile, a

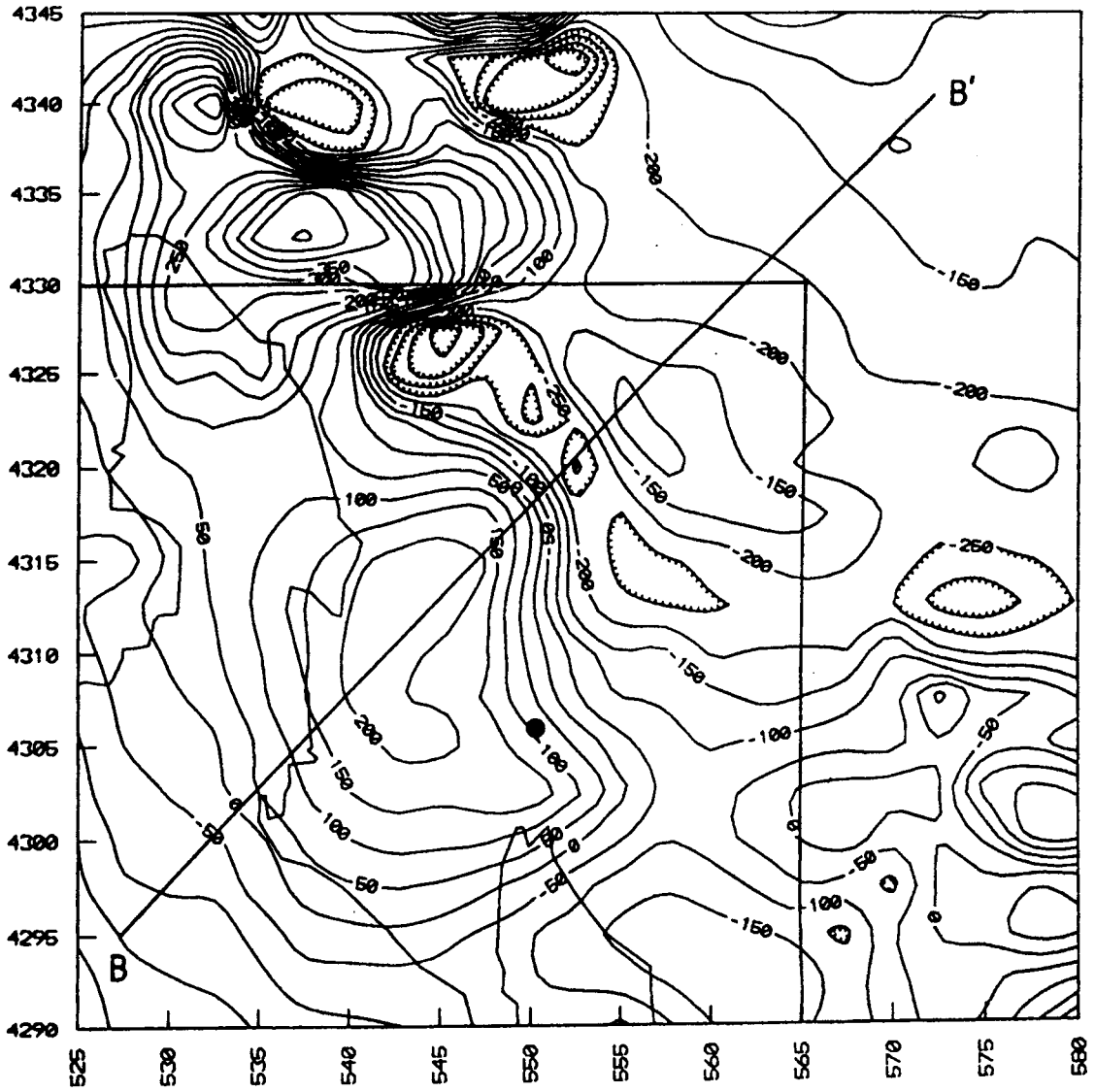

Figure 4. Aeromagnetic anomaly map. Contour interval is 50 nT. Power spectrum depth estimate method was applied to the area shown in the box. BB' is the interpreted aeromagnetic anomaly profile. Closed circle shows the location of the borehole Tuzgölü-1.

Şekil 4. Havadan manyetik anomaly haritası. Kontur aralığı 50 nT'dır. Güç spektrumu derinlik tahmini yöntemi kutu içinde gösterilen bölgeye uygulanmıştır. BB' yorumlanan gravite anomaly profilidir. İçi dolu daire Tuzgölü-1 kuyusunun yerini göstermektedir.

6 km bottom depth for the body causing the gravity anomaly can be justified. An aeromagnetic anomaly profile, (Fig. 4) chosen because it passes through approximately two-dimensional anomalies NE of the seismic section, where bottom of the inferred gabbroic body extends down to 6 km.

The borehole Tuzgölü-1 encountered granitic rocks below sandstones at a depth of 2150 m from surface. The borehole was abandoned at the depth of 2163 meters from surface. A simplified stratigraphic log of this borehole is shown in Figure 9.

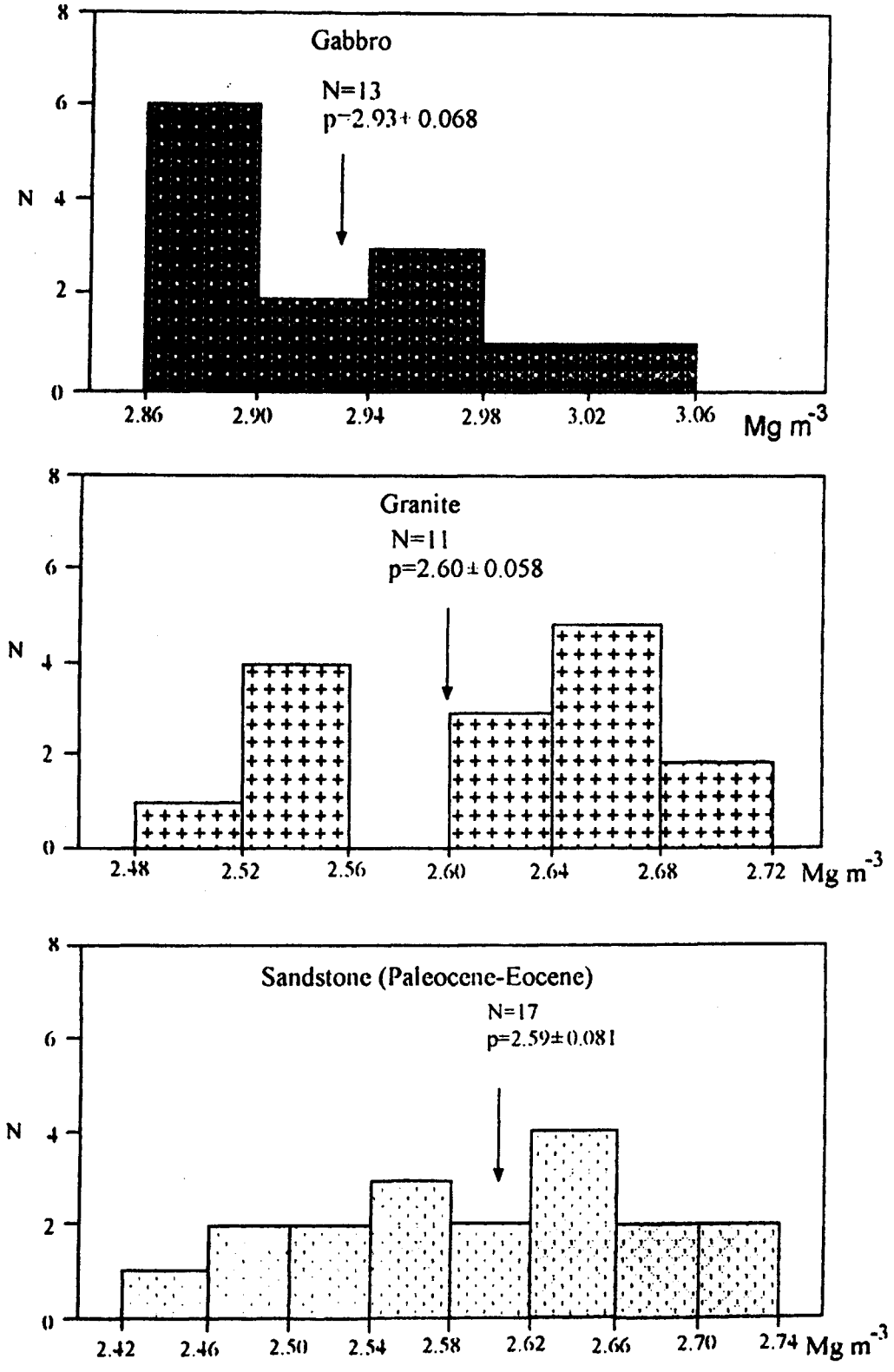

Figure 5. Density histograms of rocks from the study area.

Şekil 5. Çalışma bölgesindeki kayaçların yoğunluk histogramları.

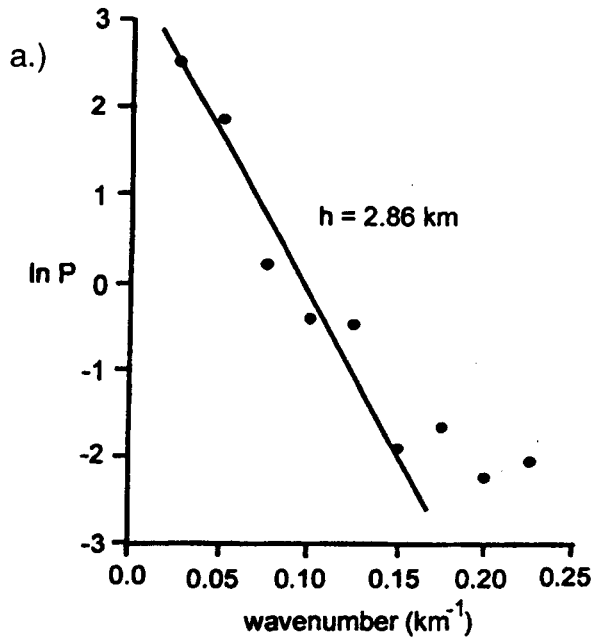

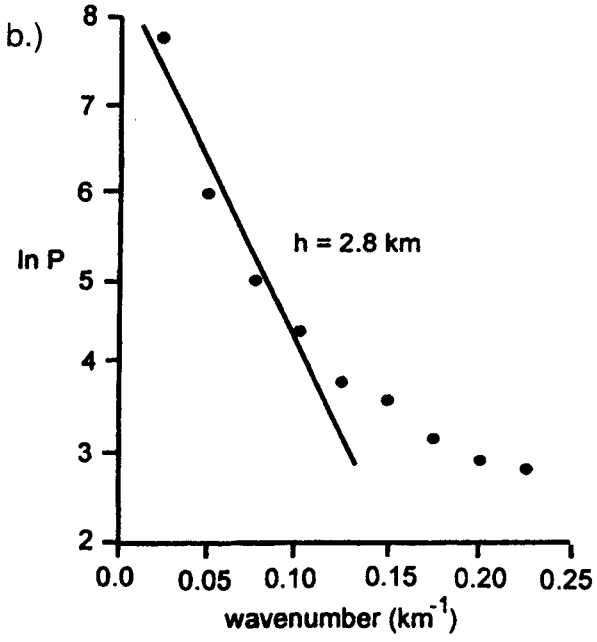

Figure 6.Power spectra obtained from gravity and aeromagnetic anomalies of boxes shown in Figures 3 and 4, respectively.

Şekil 6. Üçüncü ve dördüncü şekillerdeki kutular içindeki gravite ve havadan manyetik anomalilerden elde edilen güç spektrumu.

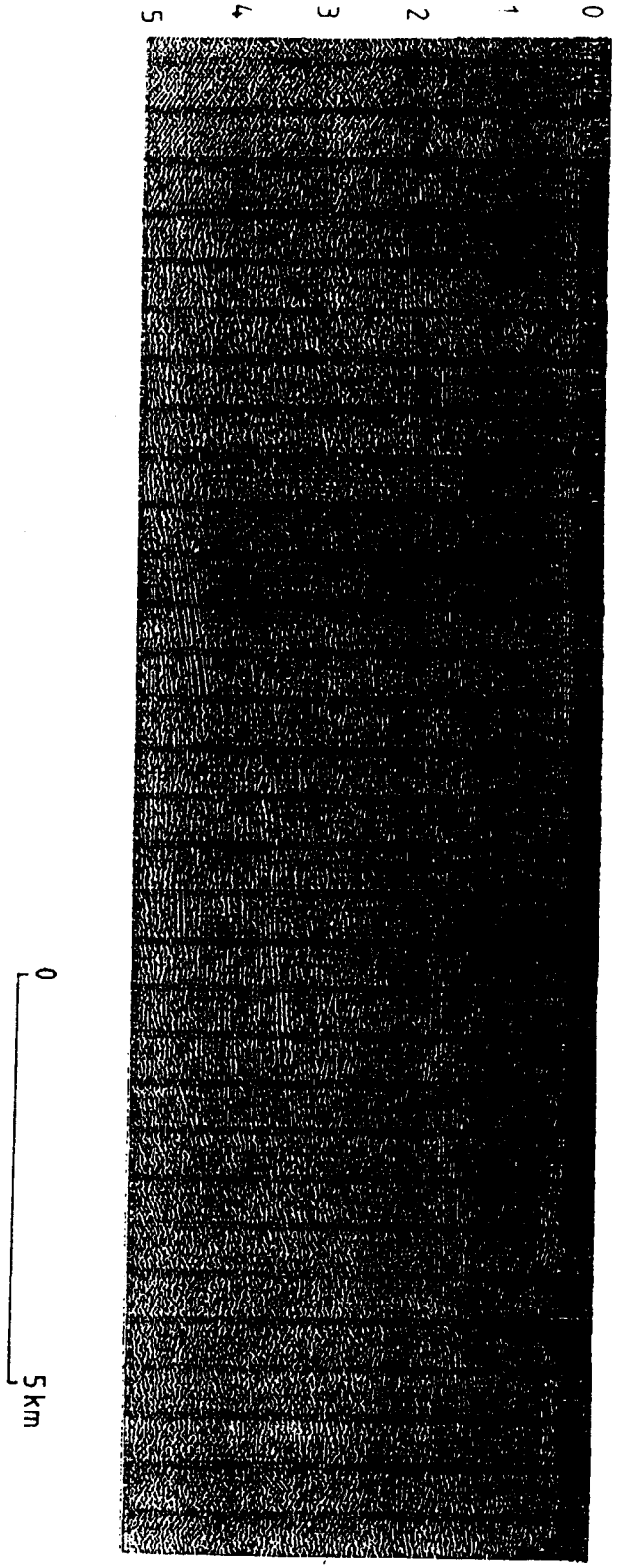

Figure 7.Seismic reflection profile DG-2012.

Şekil 7. Sismik yansıma profili DG-2012.

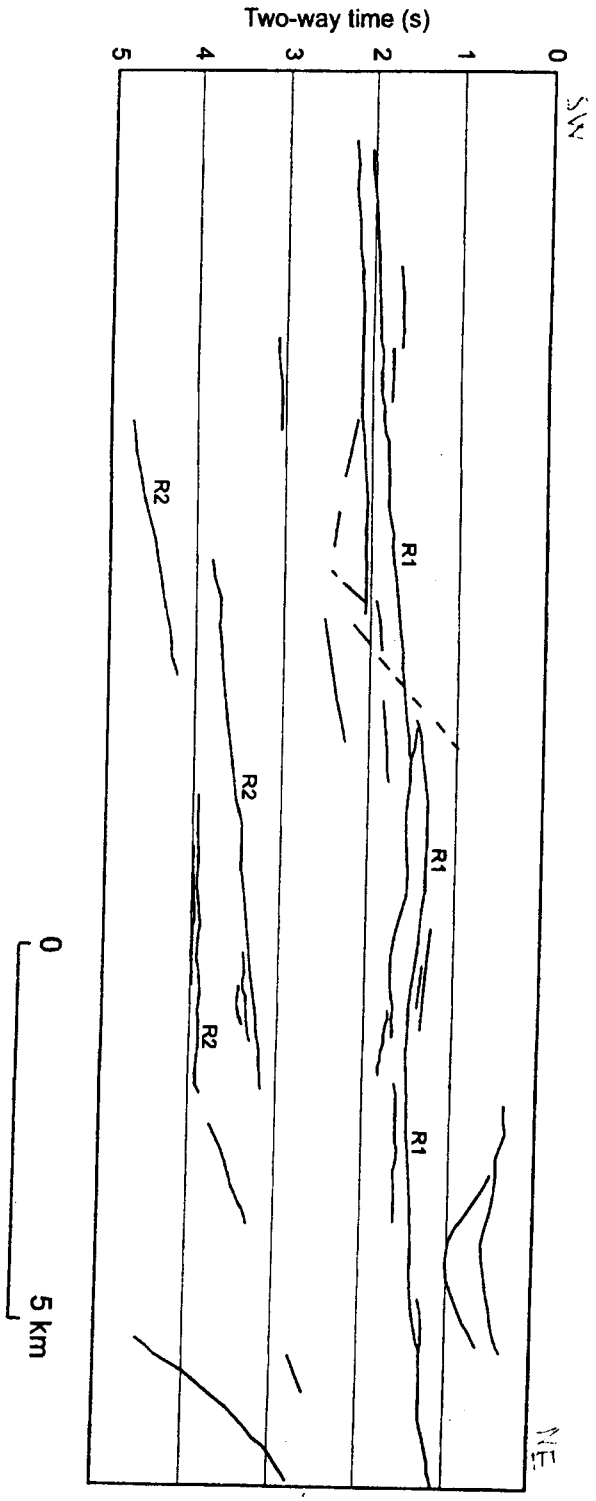

Figure 8. Line drawing of main traces of seismic profile DG-2012. For location of profile see Figure 2.

Şekil 8. Sismik profil DG-2012'nin hat çizgisellikleri. Profilin yeri için şekil 2 ye bakınız.

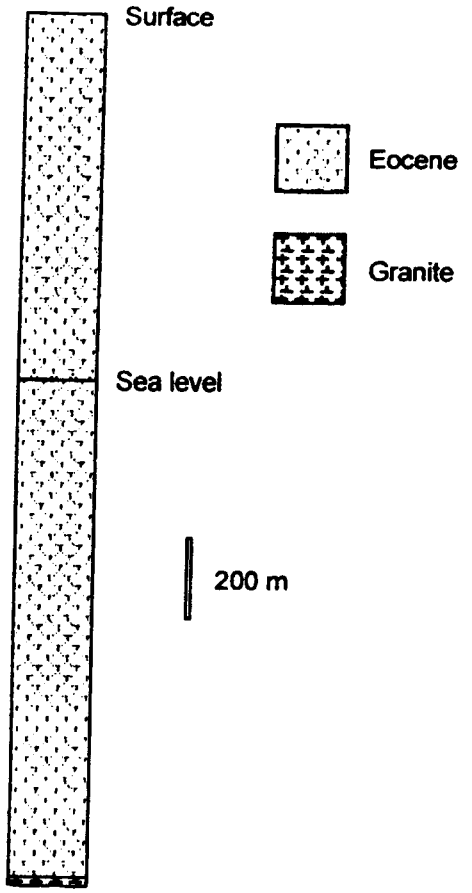

Figure 9. Simplified stratigraphic section of the borehole Tuzgölü-1.

Şekil 9. Tuzgölü-1 kuyusunun basitleştirilmiş stratigrafik kesiti.

The granite encountered at 2150 m depth suggests that the Agacoren Granitoid, which outcrops at the NE of the study area, extends underneath the Tuz Lake to SW.

TWO-DIMENSIONAL GRAVITY AND MAGNETIC MODELING

Gravity and aeromagnetic anomaly profiles were constructed (Figs. 3 and 4) using the methods of Talwani et al (1959), Talwani (1965), respectively. The gravity profile coincides with the seismic reflection line and is some 10 km SW from the borehole.

A gravity model was constructed using the borehole, seismic reflection and density data constraints. A

Table 1. Rock densities.

Çizelge 1. Kayaç yoğunlukları.

Rock type	Location	No of samples	Mean density (Mg m^{-3})	Standard deviation	Range (Mg m^{-3})
Gabbro	[•]	13	2.93	0.068	2.87-3.02
Granite	[x]	11	2.60	0.058	2.49-2.71
Sandstone (Paleocene-Eocene)	[+]	17	2.59	0.081	2.42-2.72

Table 2. Rock susceptibilities.

Çizelge 2. Kayaç suseptibiliteleri.

Rock type	Location	No of samples	Maximum susc. x 10^3, SI	Standard deviation x 10^3, SI
Gabbro	[•]	13	87.9	25
Granite	[x]	11	6.3	1.7
Sandstone (Paleocene-Eocene)	[+]	14	1.0	0.5

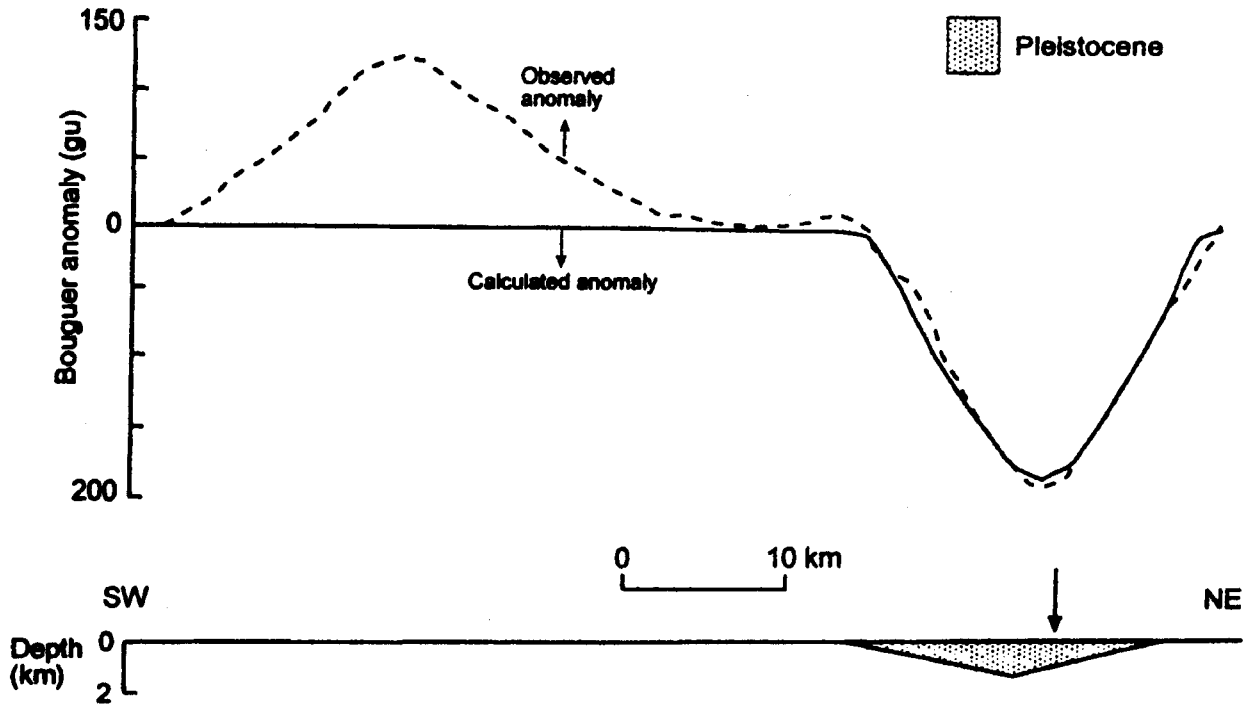

Figure 10. Interpreted two-dimensional gravity anomaly profile AA' shown in Figure 3 including only the Kızılırmak River Basin. Arrow shows the location of the Kızılırmak river.

Şekil 10. Üçüncü şekilde görülen gravite anomali profili AA' nin yalnız Kızılırmak Nehri Havzası içeren iki-boyutlu yorumu. Ok Kızılırmak nehrinin yerini göstermektedir.

low gravity anomaly at the NE end of the profile is thought to arise from Kızılırmak River Basin and can be simulated with a low density fillings (Pleistocene) (Fig. 10). However, gravity high at the SW end of the profile cannot be explained with the existing geological and gravity data. One explanation is that, if the strong reflection R1 seen in the seismic profile is attributed to the gabbroic rocks, a high gravity anomaly can be explained. Therefore, gravity model has been modified with the inclusion of a gabbroic intrusive body in the model. A density of 2.93 Mg m^{-3} has been used in the gravity model for the gabbroic body as suggested by density measurements (Table 1). A good agreement was then obtained with the observed and calculated gravity anomalies when the bottom of the gabbroic body was extended down to 6 km depth (Fig. 11). The granite found in the borehole does not affect this interpretation as the densities of the granite and surrounding Paleocene-Eocene formations close to each other (Fig. 5).

An aeromagnetic model has also been constructed about 10 km north and parallel to the gravity anomaly profile (AA') and coincides with the seismic profile. The location of the aeromagnetic anomaly profile (BB') is shown in Figure 4. The only unit which exhibits high magnetization, is gabbro (Table 2). Gabbroic rocks showed maximum susceptibility of 87.9 x 10^{-3} SI. This would provide 3.3 A m^{-1} for the intensity of magnetization. This intensity of magnetization obtained by this way was used to construct aeromagnetic model and a reasonably good fit was achieved between the observed and calculated aeromagnetic anomalies (Fig. 12).

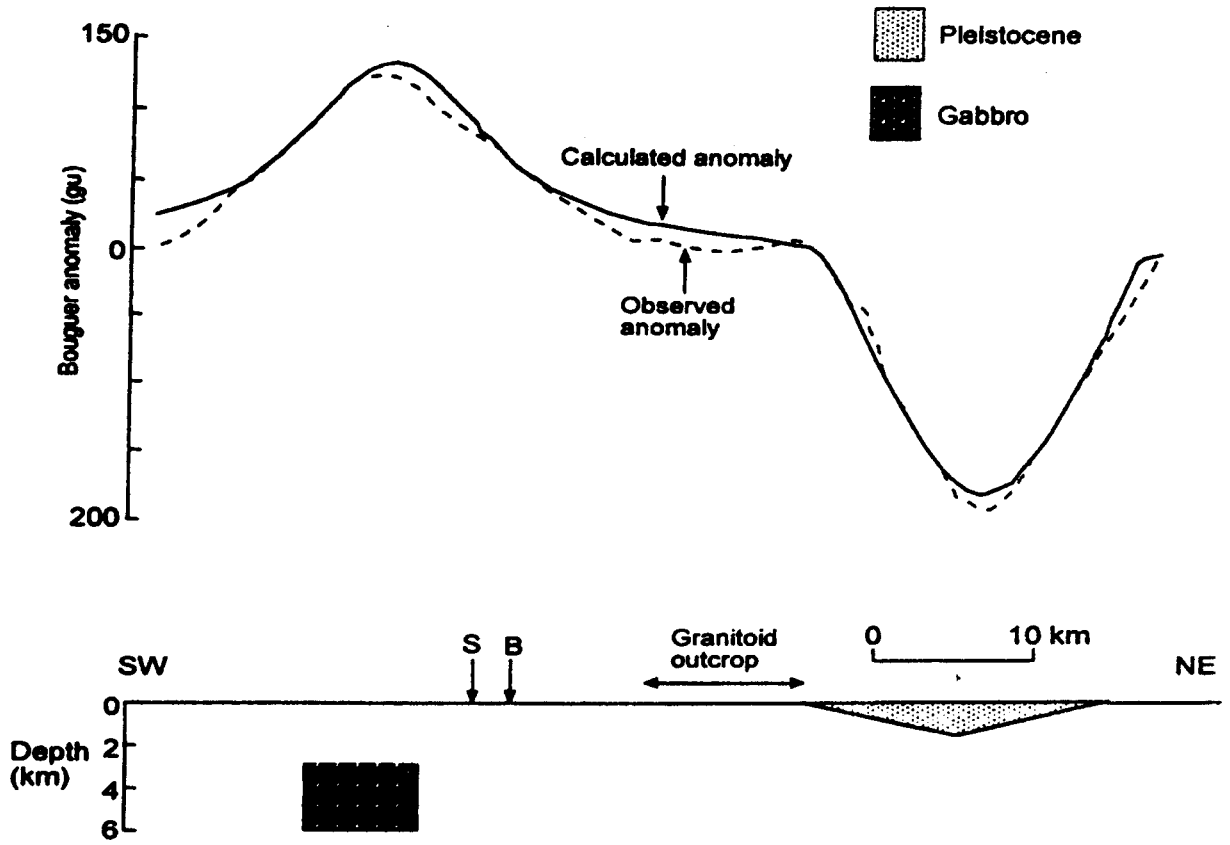

Figure 11. Interpreted two-dimensional gravity anomaly profile AA' in Figure 3 with inclusion of the gabbroic body. Arrows indicating S and B show the projected locations of the seismic section DG-2012 and borehole Tuzgölü-1.

Şekil 11. Üçüncü şekilde görülen gravite anomali profili AA' nün gabbro yapısını içeren iki-boyutlu yorumu. S ve B harflerini gösteren oklar, sismik kesit DG-2012 ve Tuzgölü-1 kuyularının yerlerini göstermektedir.

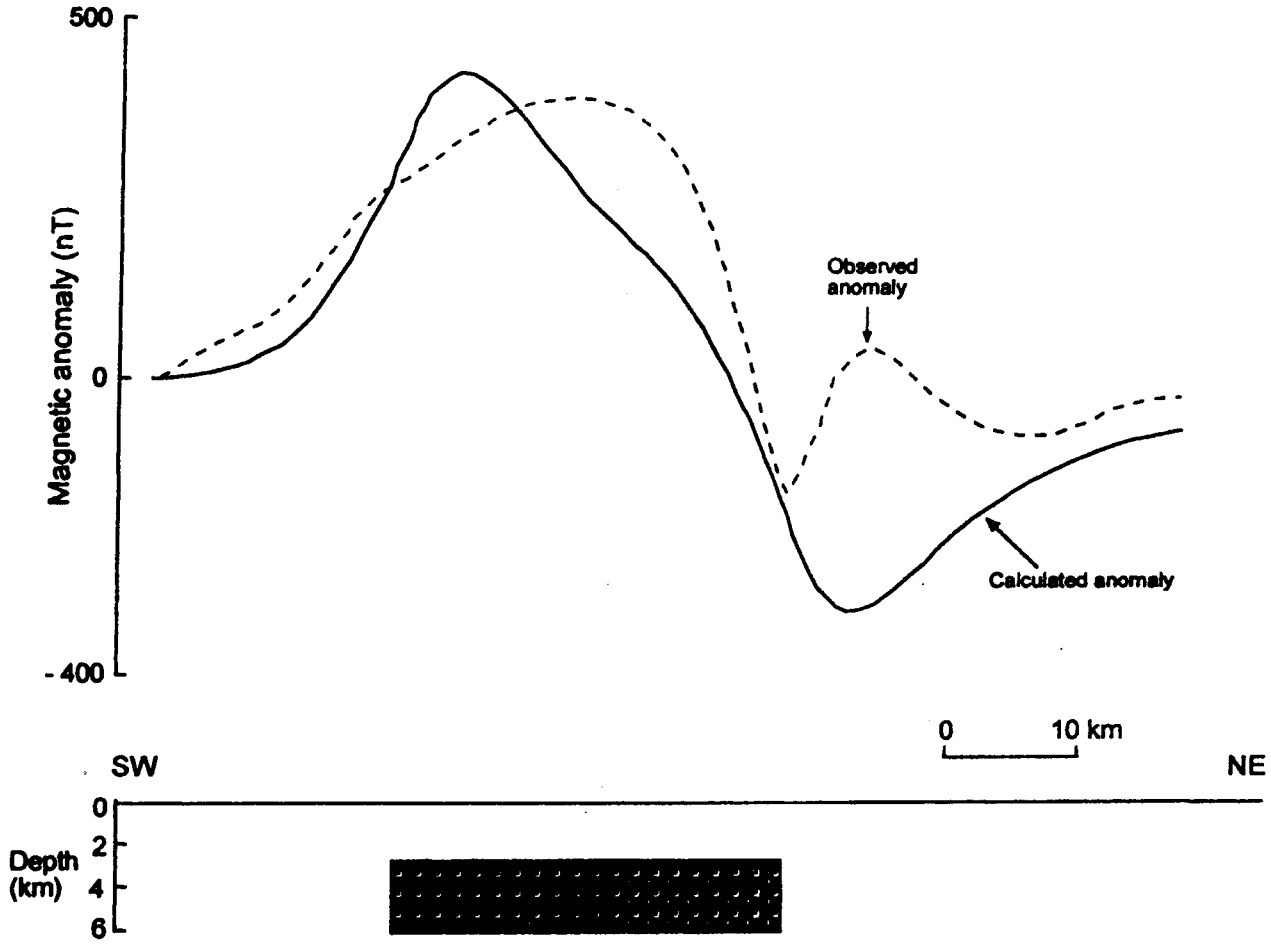

Figure 12. Interpreted two-dimensional aeromagnetic anomaly profile BB' shown in Figure 4.

Şekil 12. Dördüncü şekilde görülen havadan manyetik anomali profili BB'nün iki-boyutlu yorumu.

CONCLUSIONS

Borehole Tuzgölü-1 encountered granite at a depth of 2150 meters below the surface, suggesting that the Agacoren Granitoid extends towards and underneath the Tuz Lake. It can thus be suggested that the Agacoren Granitoid is much wider at depth than geologically observed at the surface.

Small exposures of gabbroic rocks are found at the south east corner of the study area which may be interpreted as gabbroic roots to the granitoid, extending down to mid-crustal level (Kadıoğlu et al. 1998). This appears to be suggested by the observed association of granitoids and gabbros at the surface.

Shape analysis of the gravity anomalies in Figure 3 suggests that the body causing gravity anomaly appears to be elongated in a NNE-SSW direction and thus would be wider in size than shown in gravity model in Figure 11.

The major gravity anomaly in Figure 3 appears to be aligned along almost NE-SW. One explanation is that the anomaly seems to run parallel to the main Palaeo-Tethys suture and thus the body causing the anomaly may be related to it. The densities of the granitic rocks and sandstones are very close to each other. Thus, there is no observable gravity anomaly at the contact of the granidiorite with the sandstones. Similarly, the susceptibility of these formations is too low to be distinguished magnetically. The shape of the aeromagnetic anomaly also suggests that the remanent magnetization seems to be associated with the body causing the aeromagnetic

anomaly as the peak to trough axis is not aligned towards the north magnetic pole, but aligned towards the NE. To provide further control on the remanent magnetization, the aeromagnetic anomalies in the box in Figure 4 were upward continued to 1.4 km (total height is 2 km from surface) using a computer program supplied by Banks (undated) and transformed into pseudogravity anomalies using Blakely and Simpson's (1986) algorithm (Fig. 13). The transformation was carried out using the angle of the Earth's geomagnetic field for both induced and body magnetization vectors. For correlation, the gravity anomalies of the same area shown in Figure 3 were upward continued to 2 km (Fig. 14). The purpose of upward continuation was to remove the effects of the shallow unwanted effects and to enhance the source of the deep seated body. If the transformation were performed using a declination angle of 45° E for the body magnetization (Fig. 15), the maxima of the transformed anomalies are in approximately the same locations as the maxima of the gravity anomalies of the same area in Figure 14. A similar method was also used by Kearey and Rabae (1993) to interpret the source of the Bicester magnetic anomaly in southern Britain. Thus, body causing the magnetic anomaly appears to have a remanent magnetization of 45° E declination angle and about 55° NE inclination angle. If the anticlockwise rotation of Anatolia is considered (Sanver and Ponat 1981, Rotstein 1984) the body might have gained its declination of the remanent magnetization angle greater than 135° E. This would be possible if body gained its remanent magnetization during a reverse polarity era before the anticlockwise rotation. Therefore, the body appears to be linked to the Palaeotethyan orogenic belt, as suggested above in the analysis of gravity anomalies and thus, its age older than the granitic rocks found in the region.

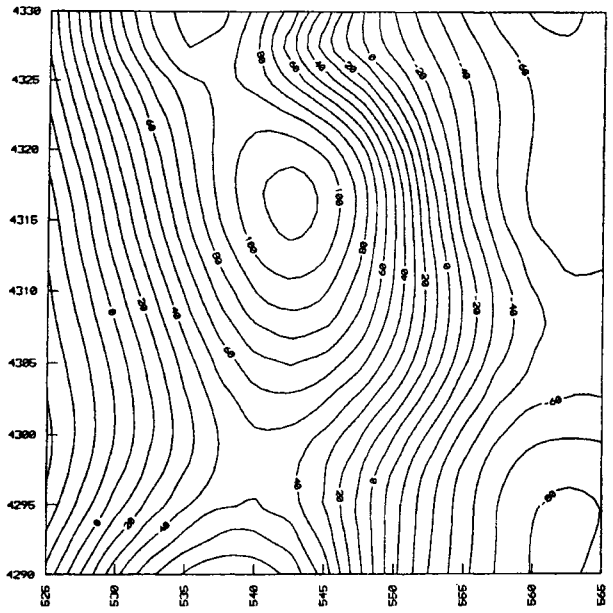

Figure 13. Pseudogravity anomalies of 1.4 km upward continued aeromagnetic anomalies (total height is 2 km) shown in Figure 4 assuming remanent magnetization is not associated with the body. Contour interval is 10 gu.

Şekil 13. Dördüncü şekilde havadan manyetik anomalilerin 1.4 km yukarı uzanımlarının (toplam yükseklik 2 km'dir) yapmagravite anomalileri. Yapının kalıntı mıknatıslanma içermediği öngörülmektedir. Kontur aralığı 10 gu'dur.

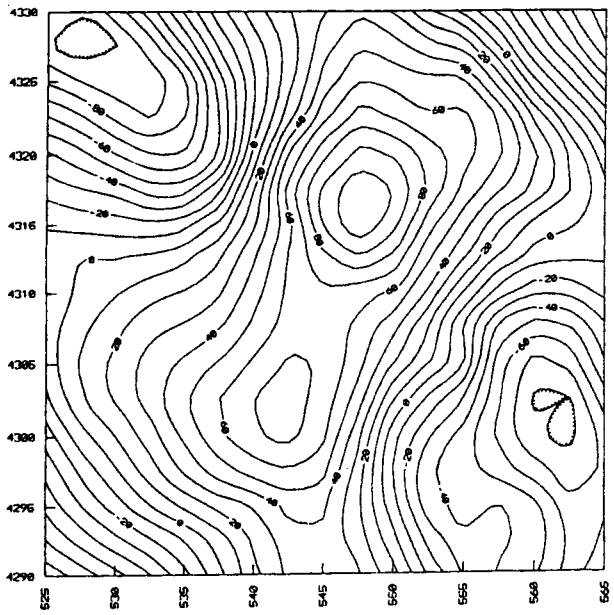

Figure 14. 2 km upward continued gravity anomalies shown by box in Figure 3. Contour interval is 10 gu.

Şekil 14. Üçüncü şekilde kutu içinde görülen bölgenin 2 km yukarı uzanım anomalileri. Kontur aralığı 10 gu'dur.

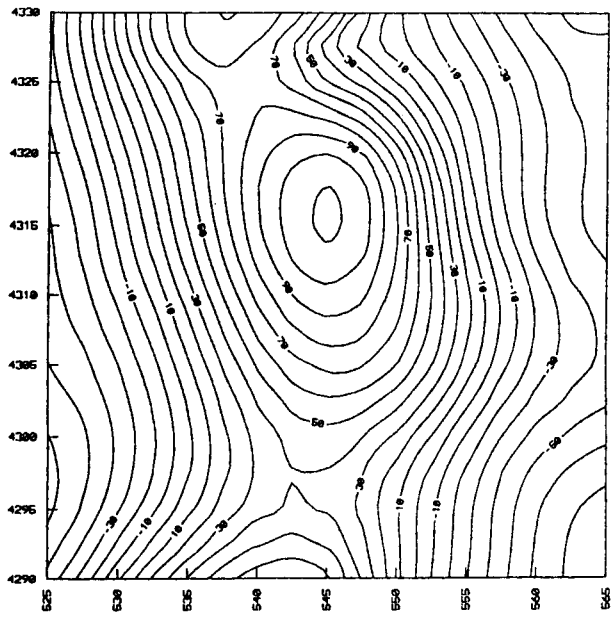

Figure 15. Pseudogravity anomalies of the aeromagnetic anomalies shown in Figure 4 assuming declination angle of the total field is 45° E. Contour interval is 10 gu.

Şekil 15. Dördüncü şekilde verilen havadan manyetik anomalilerin 1.4 km yukarı uzanımlarının yapma-gravite anomalileri. Toplam mıknatıslanmanın sapma açısı 45° D'dur. Kontur aralığı 10 gu'dur.

ACKNOWLEDGMENTS

The authors thank the General Directorates of Mineral Research and Exploration, and Petroleum Affairs Companies of Turkey for the release of the gridded potential field data, and for provision of seismic reflection profile DG-2012 and stratigraphic section of Tuzgölü-1 borehole, respectively.

REFERENCES

Ateş, A., Kearey, P. and Tufan, S. 1999. New gravity and magnetic anomaly maps of Turkey, Geophysical Journal International, 136, 499-502.

Baldwin, R. T. and Langel, R. 1993. Tables and maps of the DGRF 1985 and IGRF 1990. International union of geodesy and geophysics association of geomagnetism and aeronomy, IAGA Bulletin, No: 54, pp.158.

Banks, R.J. (Undated). Two dimensional data analysis using a library of Fortran-IV subroutines. Report, University of Lancaster, 36pp.

Bingöl, E. 1989, 1:2,000,000 scale geological map of Turkey, Publication of General Directorateof Mineral Research and Exploration, of Turkey.

Blakely, R. J. and Simpson, R. W., 1986, Approximating edges of source bodies from magnetic or gravity anomalies, Geophysics, 51, 1494-1498.

Erentöz, C. and Ketin, İ., 1961, Geological Map of Turkey, 1/500.000 Kayseri sheet, Publication of General Directorate of Mineral Research and Exploration of Turkey.

Hutchison, R. D., Lucarelli, L.B. and Hartman, R.R. 1962. Türkiye'nin müntehap sahalarında maden kaynaklarının kıymetlendirilmesi hakkında havadan istikşaf programı. Publication of General Directorate of Mineral Research and Exploration of Turkey, Field-III, no.110.

Görür, N., Oktay, F.Y., Seymen, I. and Şengör, A.M.C., 1984. Palaeotectonic evolution of the Tuzgölü basin complex, central Turkey: Sedimentary record of a Neo-Tethyan closure. In geological evolutionof the eastern Mediterranean. J.E.Dixon and Robertson, A.H.F. (eds.) Geol. Soc. Lond. spec. publ., 17, 467-482.

Kadıoğlu, Y. K., Ateş, A. and Güleç, N. 1998. Structural interpretation of gabbroic rocks in Agacoren Granitoid, central Turkey: field observations and aeromagnetic data, Geological Magazine, 135, 245-254.

Kearey, P. and Rabae, A. M. 1993. The source of the Bicester magnetic anomaly, Geological Journal, 28, 191-203.

Ketin, İ. 1966. Tectonic units of Anatolia (Asia Minor). Bulletin of the Mineral Research and Exploration Company of Institute, 66, 23-34.

Rotstein, Y. 1984. Counterclockwise rotation of the Anatolian Block, Tectonophysics, 108, 71-92.

Sanver, M. and Ponat, E. 1981.Kırşehir ve dolaylarına iliskin paleomanyetik bulgular. Kırşehir Masifinin

rotasyonu, İstanbul Yerbilimleri, 2, 231-238,

Spector, A. and Grant, F. S. 1970. Statistical models for interpreting aeromagnetic data. Geophysics, 35, 293-302.

Şengör, A.M.C. and Yılmaz, Y. 1981. Tethyan evolution of Turkey: a plate tectonic approach, Tectonophysics, 75, 181-241.

Talwani, M. 1965. Computation with the help of a digital computer of magnetic anomalies caused by bodies of arbitrary shape. Geophysics, 30, 797-817.

Talwani, M., Worzel, J.L. and Landisman, M. 1959. Rapid gravity computations for two-dimensional bodies with application to the Mendocino Submarine Fracture zone. Journal of Geophysical Research, 64, 49-59.